

# IMPLEMENTATION AND VALIDATION OF CHF MODELS IN THE TWO-PHASE FLOW POROUS MEDIA CODE TWOPORFLOW

V. Jáuregui Chávez, U. Imke, J. Jiménez and V. Sánchez-Espinoza

Institute of Neutron Physics and Reactor Technology, Karlsruhe Institute of Technology, Hermann von Helmholtz Platz 1, 76344 Eggenstein-Leopoldshafen  
veronica.chavez@partner.kit.edu; uwe.imke@kit.edu; javier.jimenez@kit.edu; victor.sanchez@kit.edu

## ABSTRACT

TWOPORFLOW is a thermal-hydraulics simulation tool currently under development at the Institute of Neutron Physics and Reactor Technology (INR) of the Karlsruhe Institute of Technology (KIT). It has the capability to simulate single- and two-phase flow in a structured or unstructured porous medium using a flexible 3-D Cartesian geometry. TWOPORFLOW calculates the transient or steady state (pseudo transient) solution of the mass, momentum and energy conservation equations for each fluid, with a semi-implicit continuous Eulerian type solver.

It was originally developed for simulation of the thermal-hydraulic phenomena inside micro-channel devices. TWOPORFLOW is capable of simulating simple 1-D geometries (like heated pipes), fuel assemblies resolving the sub-channel flow between rods or a whole nuclear core using a coarse mesh. Several closure correlations are implemented in order to model the heat transfer between solid and coolant, phase change, wall friction as well as liquid-vapor momentum coupling.

One of the most important, as well as the most difficult phenomenon to simulate, is Critical Heat Flux (CHF) in fuel bundles. Local damage of the heated surfaces may occur if the CHF is exceeded. Hence, it is important to have an accurate prediction of CHF depending on several flow parameters and boundary conditions. A large number of empirical correlations have been developed to predict CHF at different geometries and under different flow conditions. The extension of TWOPORFLOW to simulate accurately CHF phenomena has been done through the implementation of Biasi and Bowring correlations. This work presents the technique implementation and performed validation of those different CHF models using several well-known test data e.g. the BFBT benchmark.

## KEYWORDS

TWOPORFLOW, Critical Heat Flux, BFBT benchmark, Critical power, Porosity.

## 1. INTRODUCTION

The CHF is a physical phenomenon who leads to the substantial deterioration of the heat-transfer coefficient of the two-phase flow [1]. Two different kinds of CHF conditions are important. In Pressurized Water Reactors (PWR), Departure of Nucleate Boiling (DNB) appears, when, in the surface of the structure, a continuous vapor film in bubbly flow strongly decreases the heat transfer coefficient. Dry-out by full evaporation of the liquid film in annular flow can occur in Boiling Water Reactors (BWR).

This work is focused on the improvement and validation in the simulation of Dry-out using the in-house code TWOPORFLOW which uses a porous media approach to solve in 3D a system of six conservation

equations with a semi implicit transient numerical procedure based on the implicit continuous Eulerian (ICE) method [2]. In porous media, the rod and structures are seen as blocking areas and volumes with free space through which liquid or gas can pass. In TWOPORFLOW it is possible to simulate a structured (calculating the porosity base in the dimensions of the structures inside the sub-channel where  $porosity = \phi = \text{flow area} / \text{total area}$ ) and unstructured (knowing the porosity of the medium) porous medium. Figure 1 shows examples of porosities.

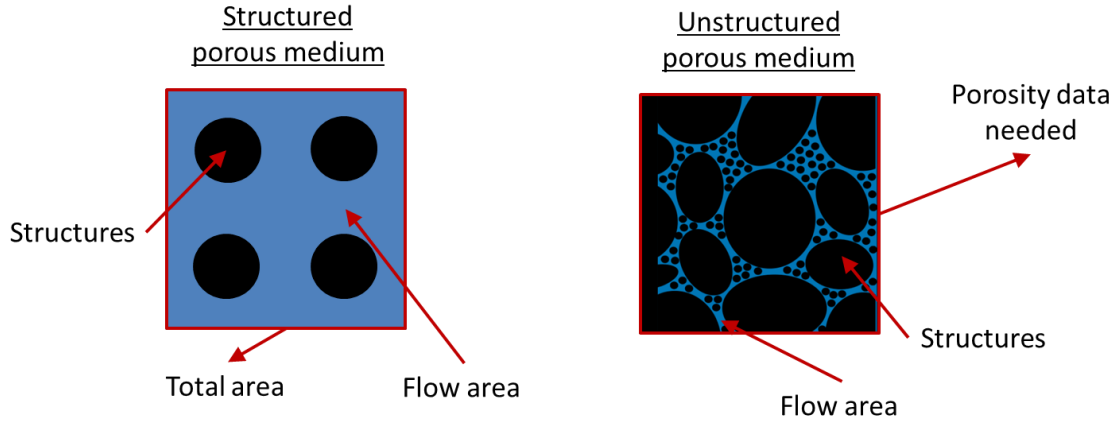


**Figure 1. Structured and unstructured porosity medium.**

The code is capable of simulating the different pre-CHF heat transfer regimes, i.e. forced convection, sub-cooled boiling and saturated boiling. But a method to calculate CHF was missing in TWOPORFLOW. Hence, two CHF correlations have been added to the code, the correlations from Biasi et al., [3] and Bowring [4] derived based on general circular tube geometry.

To validate the implemented correlations, 151 steady state experiments from NUPEC BWR Full-size Fine-mesh Bundle Test (BFBT) benchmark [5] are used. The experiments were performed in representative BWR-assembly geometries with a fuel rod arrangement of 8 x 8 and a central water rod having a larger diameter. CHF correlations and conditions of those tests will be described in the subsequent sections.

## 2. DESCRIPTION OF CHF CORRELATIONS

Correlations were developed based on 4551 [3] (Biasi) and 3800 [4] (Bowring) measured data. All those experiments were performed under a limited range of boundary conditions. The validity range of these correlations are shown in Table I

**Table I. Validity range for the application of the CHF correlations.**

Correlation	Validity range
<b>Biasi</b>	Tube diameter = 0.0030-0.0375 m
	Tube longitude = 0.2-6.0 m
	Pressure = 0.27 – 14 MPa
	Mass flux = 100 – 6000 kg/m <sup>2</sup> s
	Flow quality = 1/(1+ $\rho_l/\rho_g$ ) to 1
<b>Bowring</b>	Tube diameter = 0.002 – 0.045 m
	Tube longitude = 0.15 – 3.7 m
	Pressure = 0.2 – 19.0 MPa
	Mass flux = 136 - 18600 kg/m <sup>2</sup> s

## 2.1 BIASI CORRELATION DESCRIPTION

CHF Biasi correlation [3] was developed for uniform tube heating with a root-mean-square (*rms*) error of 7.26% in 4551 data points, and 85.5% of the points are within +/- 10% absolute deviation. As can be seen in Eq. (1), the Biasi correlation is a function of pressure in Bars ( $p_{bar}$ ), mass flux ( $G$ ), flow quality ( $x$ ), and hydraulic diameter ( $D_H$ ). This correlation has been used in different thermal hydraulic simulation programs for nuclear applications for example in COBRA-TF [6] and TRACE [7].

If  $G < 300 \text{ kg/m}^2\text{s}$ :

$$q''_{cr} = (15.048e^7)(100D_H)^{-n}G^{-0.6}H(p_{bar})(1 - x) \quad (1)$$

$$H(p_{bar}) = -1.159 + 0.149p_{bar} \exp(-0.019p_{bar}) + 9p_{bar}(10 + p_{bar}^2) \quad (2)$$

If  $G > 300 \text{ kg/m}^2\text{s}$ :

$$q''_{cr} = (2.764e^7)(100D_H)^{-n}G^{-1/6}(1.468F(p_{bar})G^{-1/6} - x) \quad (3)$$

$$F(p_{bar}) = 0.7249 + 0.099p_{bar}\exp(-0.032p_{bar}) \quad (4)$$

$$n = \begin{cases} 0.4, D_H \geq 0.01 \text{ m} \\ 0.6, D_H < 0.01 \text{ m} \end{cases} \quad (5)$$

## 2.2 BOWRING CORRELATION DESCRIPTION

Bowring correlation [4] was developed for round tubes with a uniform axial heat flux. The *rms* error in this correlation is 7% with 3800 data points. The correlation is a function of mass flow, pressure in Pascals ( $p_R$ ), flow quality, hydraulic diameter, and inlet sub-cooling; and has probably the widest range of applicability in terms of pressure and mass flux [1]. The THERMIT-2 code [8] used the correlation. That is described by the following equations:

$$q''_{cr} = \frac{A - Bh_{fg}x}{C} \quad (6)$$

$$A = \frac{2.317 \left( \frac{h_{fg} D_H G}{4} \right) F_1}{1 + 0.0143 F_2 D_H^{1/2} G} \quad (7)$$

$$B = \frac{D_H G}{4} \quad (8)$$

$$C = \frac{0.077 F_3 D_H G}{1 + 0.347 F_4 \left( \frac{G}{1356} \right)^n} \quad (9)$$

For  $p_R < 1 \text{ MPa}$ :

$$\begin{aligned} F_1 &= \frac{p_R^{18.942} \exp[20.89(1 - p_R)] + 0.917}{1.917} \\ F_2 &= \frac{F_1}{\left( \frac{p_R^{1.316} \exp[2.444(1 - p_R)] + 0.309}{1.309} \right)} \\ F_3 &= \frac{p_R^{17.023} \exp[16.658(1 - p_R)] + 0.667}{1.667} \\ F_4 &= F_3 p_R^{1.649} \end{aligned} \quad (10)$$

For  $p_R > 1 \text{ MPa}$ :

$$\begin{aligned} F_1 &= p_R^{-0.368} \exp[0.648(1 - p_R)] \\ F_2 &= \frac{F_1}{p_R^{-0.448} \exp[0.245(1 - p_R)]} \\ F_3 &= p_R^{0.219} \\ F_4 &= F_3 p_R^{1.649} \end{aligned} \quad (11)$$

### 3. VALIDATION USING THE STEADY STATE BFBT CHF TESTS

#### 3.1 TEST DESCRIPTION

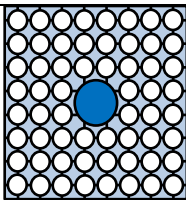
The BWR Full-size Fine-mesh Bundle Test (BFBT) Benchmark [5] was developed by the Nuclear Power Engineering Corporation (NUPEC) of Japan due the need to refine models for best-estimate thermal-hydraulic calculations based on good-quality experimental data, and that consists of two phases: Void distribution and Critical Power tests. The latter, is subdivided into steady state and transient tests. Here, the steady state tests are used first to demonstrate the TWOPORFLOW prediction capability to simulate CHF phenomenon in fuel assemblies. In total 151 experiments were performed using an 8 x 8 pin

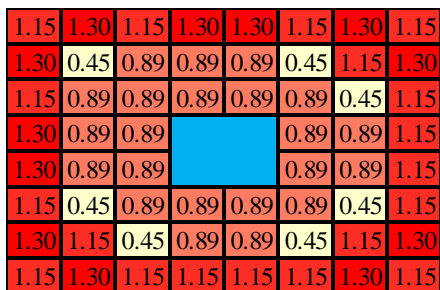
arrangement with a single central water rod. The axial heated length is 3708 mm. The boundary conditions of the experiments are listed hereafter:

- Outlet pressure: 5.5 – 8.6 MPa
- Inlet mass flux: 290 - 2000 kg/m<sup>2</sup>s
- Inlet temperature : 243 - 296 °C
- Initial power: 20 - 80 MW/m<sup>2</sup>

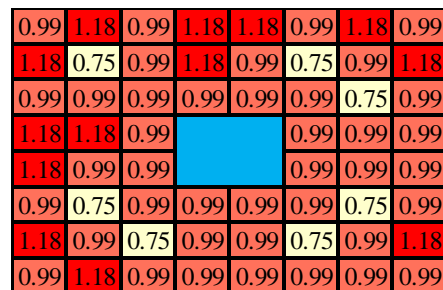
The geometry and power shape of the assemblies are shown in Table 2 and Figure 2, respectively.

**Table 2. Geometry and Power shape for test Assemblies C2A, C2B and C3.**

Item	Data		
			
Test assembly	C2A	C2B	C3
Heated rod outer diameter (mm)	12.3		
Heated rod pitch (mm)	16.2		
Water rod outer diameter (mm)	34		
Channel box inner width (mm)	132.5		
In channel flow area (mm <sup>2</sup> )	9463		
Spacer type	Ferrule		
Number of spacers	7		
Spacer pressure loss coefficients	1.2		
Spacer location (mm)	455, 967, 1479, 1991, 2503, 3015, 3527 (distance from bottom of heated length to spacer bottom face)		
Radial power shape	Figure 2 A)	Figure 2 B)	Figure 2 A)
Axial power shape	Cosine	Cosine	Inlet-peak



**A) Assemblies C2A, C3 (reactor conditions at the beginning of cycle)**



**B) Assembly C2B (reactor conditions at the middle of cycle)**

**Figure 2. Radial power distribution BFBT.**

The critical power was measured by slowly increasing the bundle power while monitoring the individual heater rod thermocouple signals measuring the local cladding temperature. The critical power was defined when the peak rod surface temperature became 14°C higher than the steady-state cladding temperature level. Dry-out was observed in the peak power rod located at the peripheral row adjacent to the channel box. The boiling transition was always observed just upstream of the spacer.

Figure 3 shows the radial and axial thermocouple positions. Each thermocouple position is identified as follows: **Rod No. – Axial location – Circumferential angle**. Measurements are located in the rods 1, 2, 4, 8, 12, 25, 26, 45, 53, 59, and 60, at different axial locations A (3521 mm), B (3009 mm), C (2497 mm), D (1985 mm), and different rotational angles. In TWOPORFLOW it is not possible to calculate the circumferential position of CHF. Due to porous medium approach such details cannot be solved.

For that reason in this study the experimental temperatures are compared with the average simulated temperatures of the structure in the sub-channel, where the CHF appears.

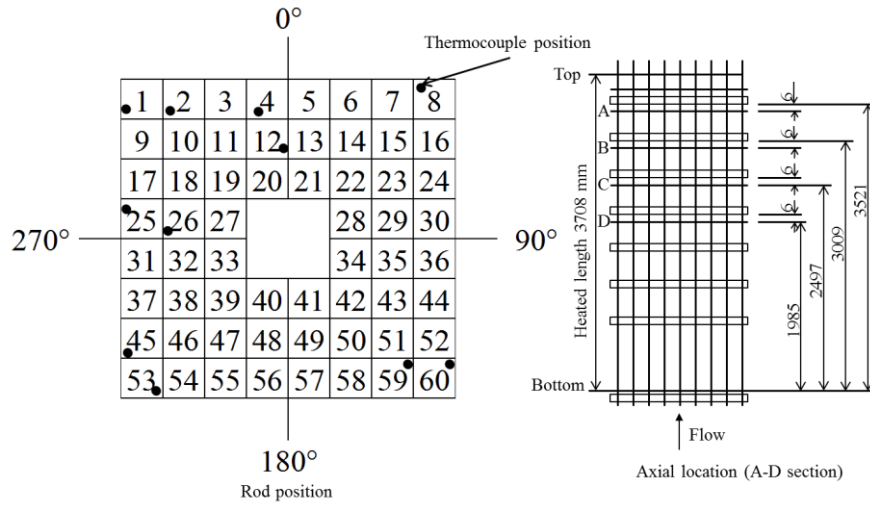


**Figure 3. Definition of thermocouple radial and axial position with the radial location of the TC (black dots).**

#### 4. SIMULATION OF BFBT BUNDLE WITH TWOPORFLOW

In TWOPORFLOW the assembly is modeled using a centered rod approach, making an arrangement of 8x8 sub-channels with 24 cells in axial direction. The pins and water rods are represented using a calculated porosity of 0.57 and 0.17 in axial direction respectively (Figure 4). In radial direction the porosity is 0.68. The heat transfer area is given by the outer radius of the fuel rods ( $140.86 \text{ m}^2$ ). The hydraulic diameters in axial direction (0.008 m corners, 0.016 m edges, 0.011 m inner sub-channels, 0.007 m water rods) and in lateral direction (0.021m) are used to calculate local pressure loss and heat transfer. The spacer grids are represented using a pressure loss coefficient of 1.2 at different heights (Table 2). The heat transfer within the fuel rod is described by a radial one dimensional heat conduction equation. The fuel pellet is divided into 8 radial nodes. The cladding is represented by two radial nodes.

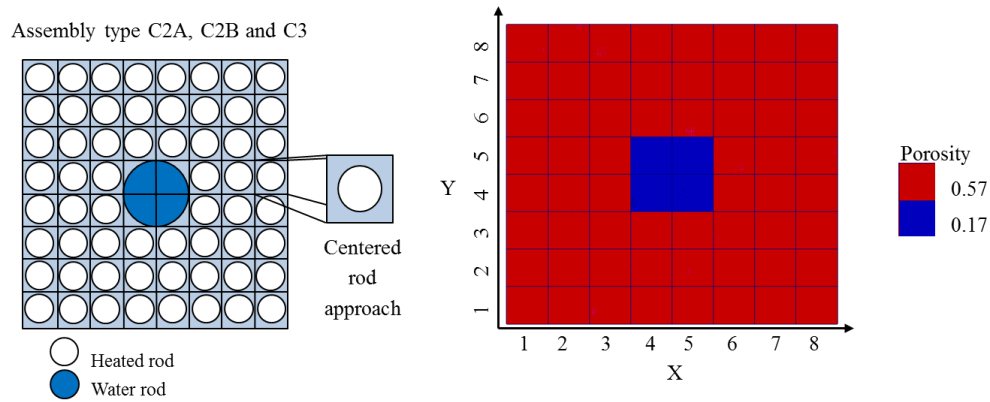


**Figure 4. Geometrical arrangement in TWOPORFLOW.**

The 151 simulations have been made using a tool developed in INR, which is capable to call TWOPORFLOW to run a set of inputs serially.

The time step is automatically calculated by the code (0.1 second for a typical case). The CPU time needed to calculate one test is about 5 minutes.

## 5. COMPARISON OF PREDICTIONS WITH MEASURED DATA

To investigate which parameter influences the quality of the CHF simulations, the ratio of simulated and measured values are plotted against mass flux. In Figure 5 each point represents one simulation. It is also observed that, for assembly C2A, an increasing mass flux results in a trend from under-prediction to over-prediction. For assembly C2A, the experiments were performed with 3 different pressures 8.6, 7.2, and 5.5 MPa, while in assembly C2B and C3 only a pressure of 7.2 MPa was applied. For the Bowring correlation, the gradient strongly depends on the pressure. The behavior of Biasi is similar, but less drastic than using Bowring.

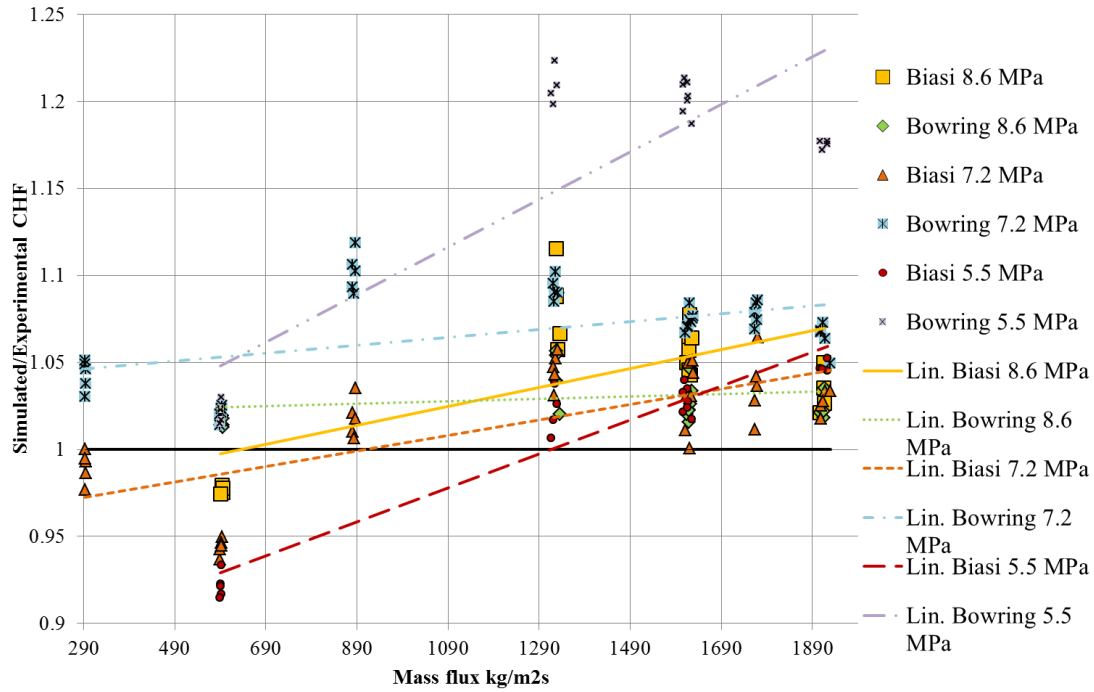


**Figure 5. Tendency of CHF prediction accuracy in relation with mass flux and pressure in assembly C2A.**

Figure 6 shows the same analysis using assemblies C2B and C3. Assembly C3 behaves like C2A, since both have the same radial power distribution. However, in C2B, the behavior changes because the power distribution influences strongly the results as well.

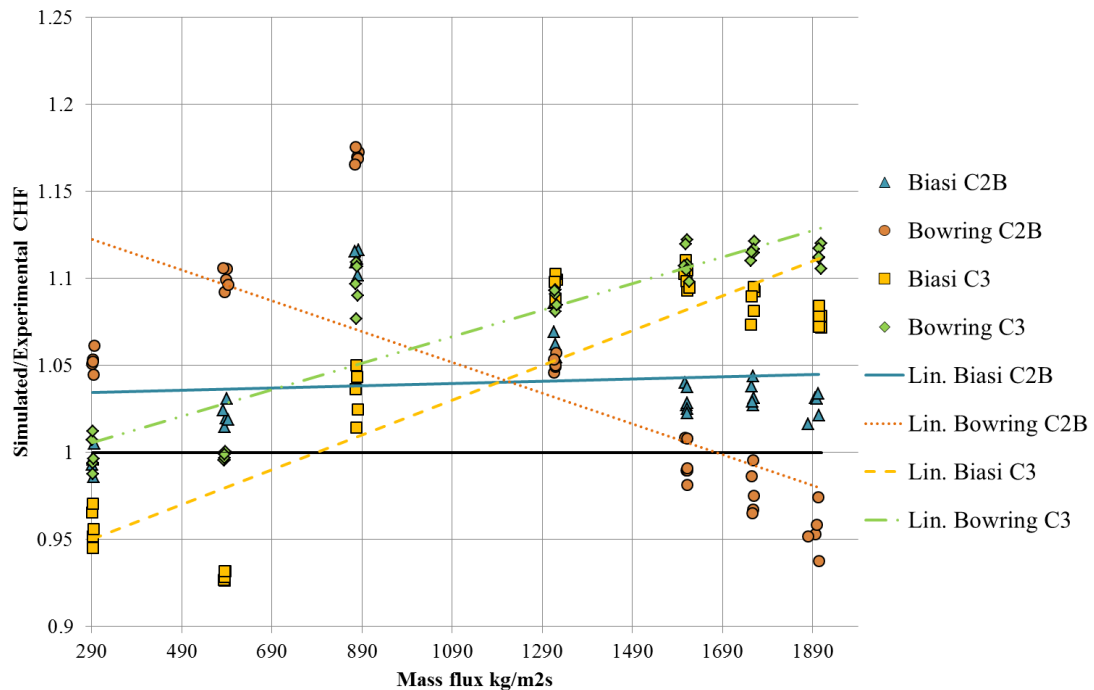


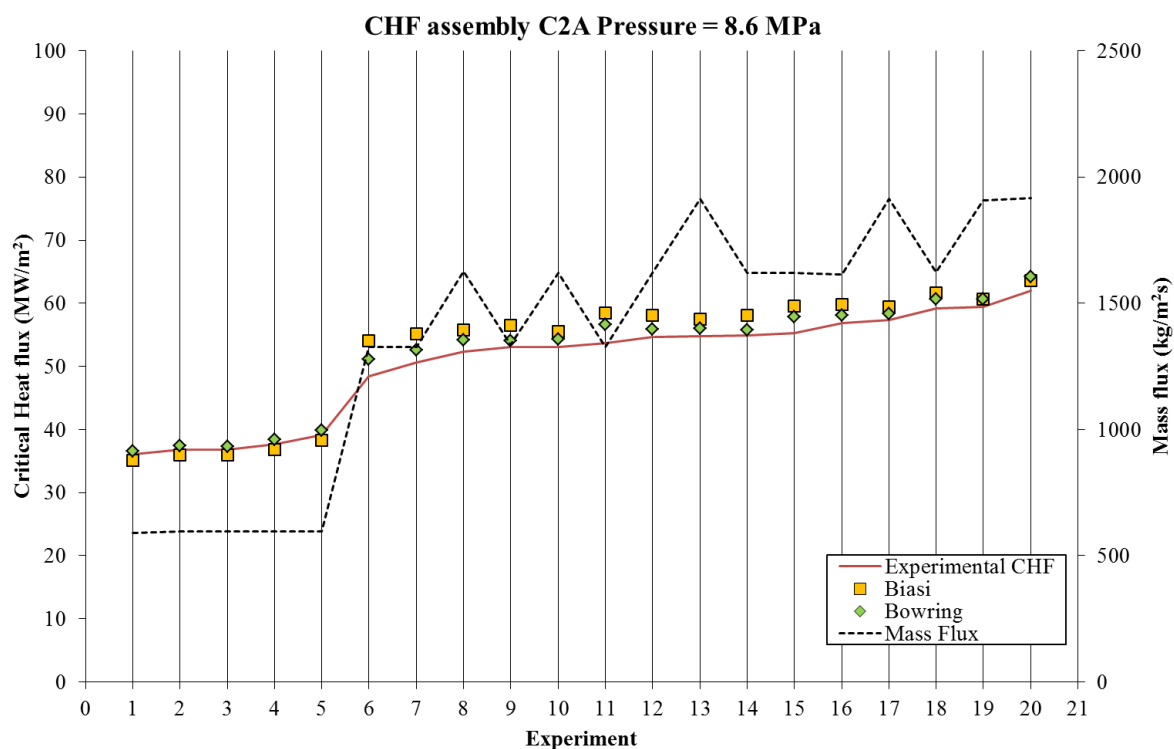
**Figure 6. Tendency of CHF prediction accuracy in relation with mass flux in assemblies C2B and C3.**



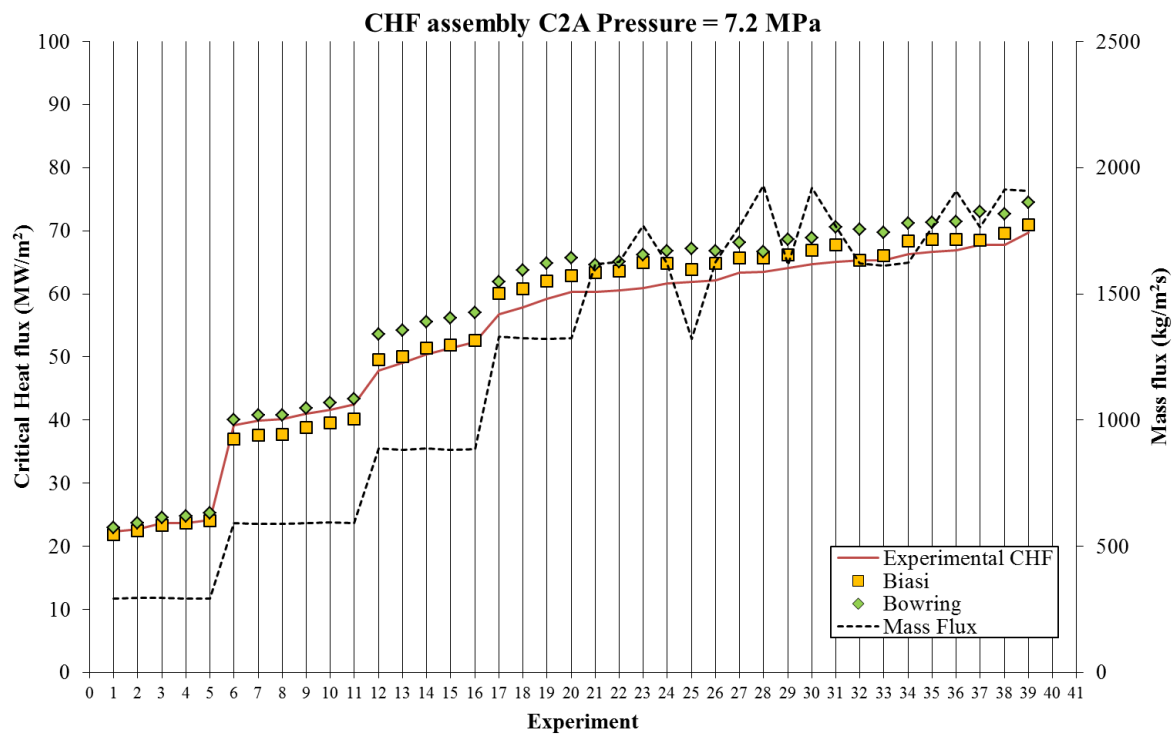
A similar study was made for initial sub-cooling, but that parameter does not show any influence in the quality of CHF simulation.

Figure 7 to Figure 11 show the relation between the experimental and calculated CHF, and mass flux. Analyzing the results, the mass flux influences the quality of the simulation results, mainly for low pressures and high mass fluxes leading to an over-prediction of CHF. Comparing Figure 7, Figure 8 and Figure 9, it is observed that the pressure condition and the power shape are much more important for the quality of the simulations.

We can compare the three different power shapes using similar conditions. Figure 8, Figure 10, and Figure 11, show that for assemblies C2A and C3, and a heat flux higher than  $60 \text{ MW/m}^2$ , both correlations overpredict the CHF in most of the cases. This does not happen with the C2B assembly.



**Figure 7. CHF assembly C2A Pressure 8.6 MPa.**



**Figure 8. CHF assembly C2A Pressure 7.2 MPa.**

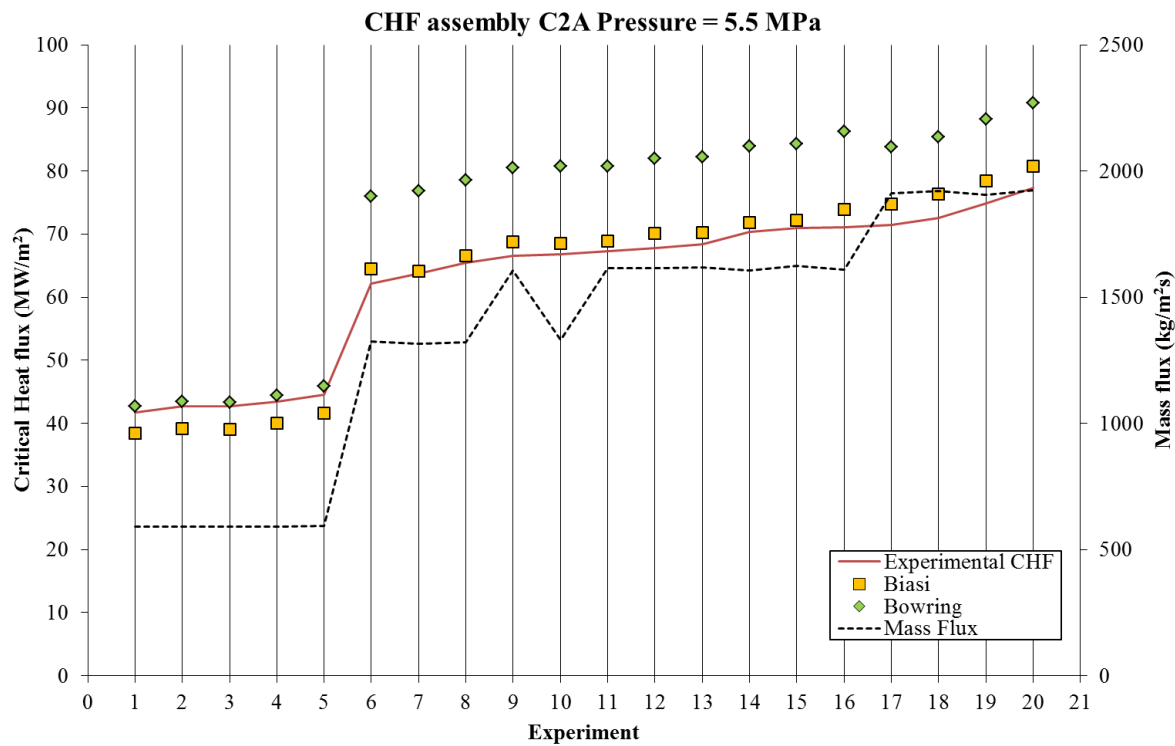


**Figure 9. CHF assembly C2A Pressure 5.5 MPa.**

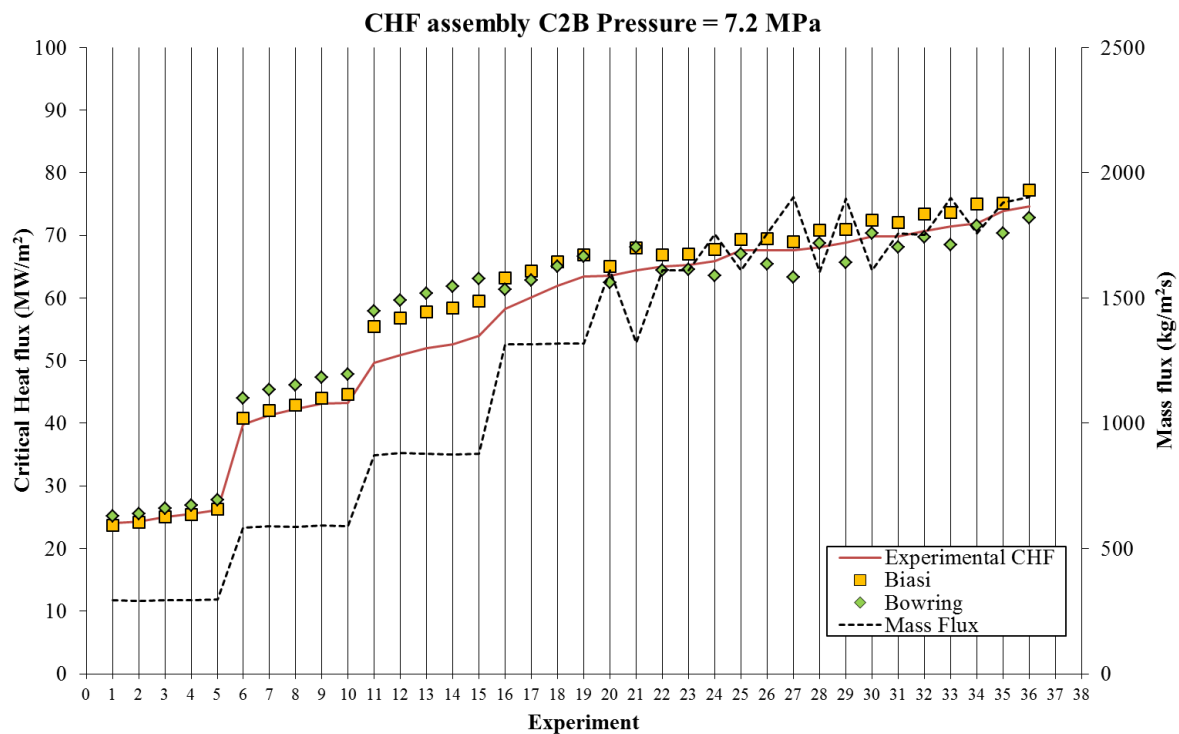


**Figure 10. CHF assembly C2B Pressure 7.2 MPa.**

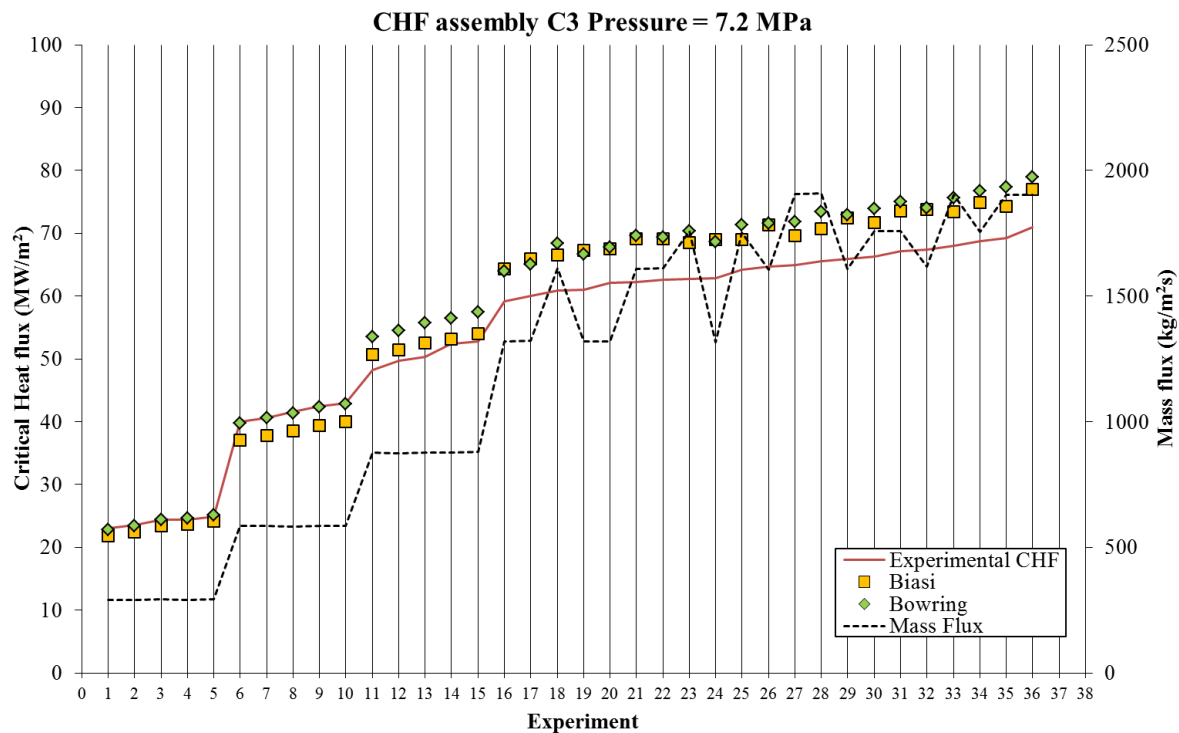


**Figure 11. CHF Assembly C3 Pressure 7.2 MPa.**

In Figure 12 the comparison between the calculated and the measured CHF in the 151 experiments is shown. The simulation results having stronger deviation from the measurement are those with a lower pressure in the Bowring correlation, which are highlighted in red in the mentioned Figure. The Biasi correlation shows a difference less than the 10% in most of the cases but nevertheless, no result is more than 20% different from the experimental values.

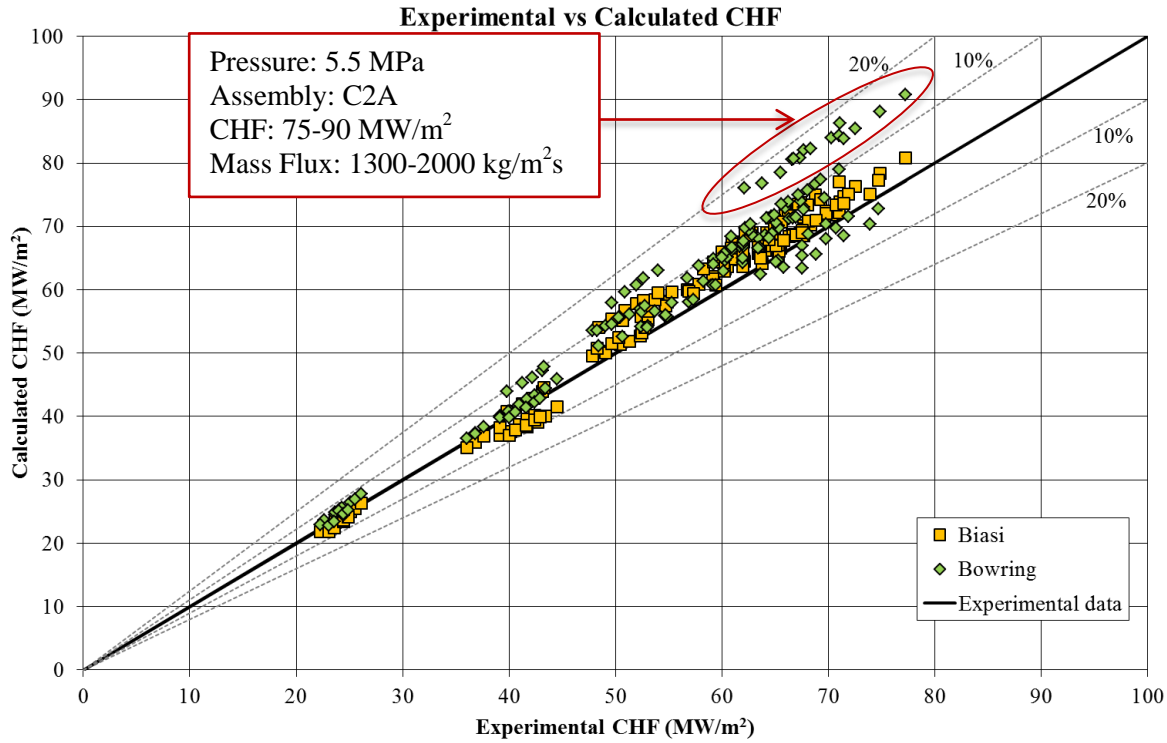


**Figure 12. Comparison between calculated and experimental CHF.**

## 6. CONCLUSIONS

Using the Bowring correlation the deviation from experimental values has a stronger dependence on pressure than when Biasi was applied, although both correlations present a strong dependence on power distribution. Most of the results obtained with Biasi are inside a deviation limit of less than 10%, while the experiments with a lower pressure are near 20% when Bowring was used. However results show a difference narrower than 20%. Both correlations can be used for investigated geometry and given boundary conditions, but it is recommended to use Biasi at low pressures (5.5 MPa or lower in this case) in TWOPORFLOW. The next step in the improvement of the CHF prediction will be the implementation and validation of the Groeneveld Look-up table [9] in TWOPORFLOW.

## ACKNOWLEDGMENTS

This work has been performed at the Institute for Neutron Physics and Reactor Technology (INR) of the Karlsruhe Institute of Technology (KIT). The authors would like to thank the Program Nuclear Safety Research of KIT for the financial support of the research topic “multi-physics methods for LWR”, as well as the German Academic Exchange Service (DAAD) and the Mexican National Commission of Science and Technology (CONACYT).

## REFERENCES

1. N. E. Todreas and M. S. Kazimi, *Nuclear Systems I: Thermal Hydraulic Fundamentals*, Taylor & Francis, United States of America (1993).
2. U. Imke, "Porous media simplified simulation of single- and two-phase flow heat transfer in micro-channel heat exchangers," *Chemical Engineering Journal*, **101**, pp. 295-302 (2004).
3. L. Biasi, G. Clerici, S. Garribba, R. Sala and A. Tozzi, "Studies on burnout, Part 3" *Energia Nucleare*, **14(9)**, pp. 530-536 (1967).
4. R. Bowring, "Simple but Accurate Round Tube, Uniform Heat Flux Dryout Correlation over the Pressure Range 0.7 to 17 MPa," U.K. Atomic Energy Authority, **no. AEEW-R-789** (1972).
5. B. Neykov, F. Aydogan, L. Hochreiter, K. Ivanov, H. Utsuno, F. Kasahara, E. Sartori, M. Martin, *NUPEC BWR Full-size Fine-mesh Bundle Test (BFBT) Benchmark. Volume I: Specifications*, OECD, Japan (2006).
6. R. K. Salko and M. N. Avramova, *COBRA-TF Sub-channel thermal-hydraulics code (CTF) Theory Manual*, Pennsylvania State University (March 2015).
7. United States Nuclear Regulatory Commission, *TRACE V5.0 Theory Manual, field equations, solution methods, and physical models*, Washington, DC, USA (2009).
8. J. Kelly, S. Kao and M. Kazimi, "THERMIT-2: A two-fluid model for Light Water Reactor subchannel transient analysis," *MIT Energy Laboratory Electric Utility Program Report No. MIT-EL-81-014*, Cambridge, Massachusetts (1981).
9. D. Groeneveld, J. Shan, A. Vasic, L. Leung, A. Durmayaz, J. Yang, S. Cheng and A. Tanase, "The 2006 CHF look-up table," *Nuclear Engineering and Design*, **vol. 237**, pp. 1909-1922 (2007).